nature communications

Article

https://doi.org/10.1038/s41467-025-61443-4

Early-life exercise extends healthspan but not lifespan in mice

Received: 18 July 2024

Accepted: 12 June 2025

Published online: 09 July 2025

Check for updates

Mengya Feng[1,2,9], Min Li[2,9], Jing Lou[2], Guiling Wu[2], Tian Gao[3], Fangqin Wu[2], Yanzhen Tan[4], Nini Zhang[2], Yong Zhao[5], Lin Zhao[6], Jia Li[2], Changhong Shi[5], Xing Zhang[2] ✉, Jiankang Liu[1,7,8] ✉ & Feng Gao[2] ✉

It is well-known that physical activity exerts health benefits, yet the potential impacts of early-life regular exercise on later-life health and lifespan remains poorly understood. Here, we demonstrate that 3 months of early-life exercise in mice results in lasting health benefits, extending healthspan, but not lifespan. C57BL/6J mice underwent swimming exercise from 1 to 4 months of age, followed by detraining for the remainder of their lives. While early-life exercise did not extend the overall lifespan, it significantly improved healthspan in both male and female mice, as evidenced by enhanced systemic metabolism, cardiovascular function, and muscle strength, as well as reduced systemic inflammation and frailty in aged mice. Multiple-organ transcriptome analyses identified enhanced fatty acid metabolism in skeletal muscles as a major feature in aged mice that underwent early-life exercise. These findings reveal the enduring long-term health benefits of early-life exercise, highlighting its pivotal role in improving healthspan.

Physical inactivity poses a major public health threat, contributing significantly to the rise of noncommunicable diseases (NCDs) and associated mortality worldwide[1,2]. The highest NCDs prevalence from physical inactivity is observed among persons who went on to develop type 2 diabetes, (overall median, 43%), followed by those eventually dying, and those developing colon cancer, coronary heart disease, and breast cancer (overall medians, 43, 43, 42, and 41%, respectively)[3]. Exercise is widely recognized as the most effective and cost-efficient intervention to promote overall health and reduce the burden of NCDs[4,5]. However, latest global estimates show that 1.4 billion adults (27.5% of the world's adult population) fall short of meeting the recommended level of physical activity[6]; and the situation is equally, if not more alarming among school-aged children and adolescents. It is estimated that the majority (81%) of boys and girls aged 11–17 years failed to meet the recommended level of physical activity[7]. In China, which constitutes one-sixth of the world's youth population, this issue is of particular concern, as the prevalence of inactivity, sedentary behavior, and smartphone addiction is on the rise[8]. These trends have been linked to an increasing incidence of NCDs[8,9]. Unfortunately, the significance of physical activity during childhood has not received sufficient attention.

Emerging evidence supports that early-life experiences and fitness affect long-term health outcomes[10]. Recent epidemiological studies highlight a positive correlation between higher levels of physical activity in childhood and enhanced aerobic fitness, elevated bone mineral density (BMD) and reduced risks of metabolic diseases, including obesity, hypertension, type 2 diabetes mellitus, and cardiac disease later in life[11–13]. We recently reported that early-life exercise

[1]Center for Mitochondrial Biology and Medicine, Key Laboratory of Biomedical Information Engineering of Ministry of Education, School of Life Science and Technology, Xi'an Jiaotong University, Xi'an, China. [2]Key Laboratory of Aerospace Medicine of the Ministry of Education, School of Aerospace Medicine, Fourth Military Medical University, Xi'an, China. [3]Center of Health Management, Tangdu Hospital, Fourth Military Medical University, Xi'an, China. [4]Department of Thoracic Surgery, Shaanxi Provincial People's Hospital, The Third Affiliated Hospital of Xi'an Jiaotong University, Xi'an, China. [5]Laboratory Animal Center, Fourth Military Medical University, Xi'an, China. [6]Cardiometabolic Innovation Center, Ministry of Education, Department of Cardiology, First Affiliated Hospital of Xi'an Jiaotong University, Xi'an, China. [7]School of Health and Life Sciences, University of Health and Rehabilitation Sciences, Qingdao, China. [8]Department of Dermatology, First Affiliated Hospital of Xi'an Jiaotong University, Xi'an, China. [9]These authors contributed equally: Mengya Feng, Min Li.
✉e-mail: zhangxing@fmmu.edu.cn; j.liu@mail.xjtu.edu.cn; fgao@fmmu.edu.cn

enhances anti-inflammatory immunity in middle-aged male mice[14]. These findings suggest the enduring potential of early-life physical activity to positively impact human health over time. However, the precise influence of early-life exercise on adult health remains uncertain, given that individuals with higher physical activity during childhood tend to sustain elevated activity levels into adulthood[15]. In addition, due to the relatively short follow-up periods in human studies, it is unknown whether early-life exercise confers lifelong benefits. In this study, we investigated the impact of early-life exercise alone on overall health in later life in mice and found that 3-month exercise during early-life exerts significant long-term health benefits, improving healthspan in both male and female mice.

Results

Early-life exercise does not extend lifespan in both male and female mice

Male and female C57BL/6J mice were subjected to either sedentary conditions or swimming exercise (90 min per day for 3 months) at 1–4 months of age and then reared without exercise training in the rest of the life (Fig. 1a). In female mice, early-life exercise resulted in increased body weight from 4 to 29 months of age. Conversely, in male mice, early-life exercise led to a reduction in body weight at 4 months of age, but with no significant impact on body weight at other time points (Fig. 1b, c). Early-life exercise did not extend overall survival by Tarone-Ware and Gehan-Breslow-Wilcoxon tests in both male and female mice (Supplementary Table 1), although it seemed to increase day-by-day survival within a narrow timeframe throughout the lifespan, as indicated by daily chi-square test, with a more obvious effect observed in females (Supplementary Fig. 1). However, early-life exercise increased the maximum lifespan (lifespan of the longest lived 5% of individuals) in both male (34.08 vs. 29.5 months) and female (36.25 vs. 32.86 months) mice, without substantial difference in median lifespan (Fig. 1d, e, Supplementary Table 1). These results suggested that early-life exercise had no significant impact on the median and overall lifespan in mice.

Early-life exercise increased lean mass and decreased circulating insulin in aged mice

Given that metabolic alterations accumulated over time are closely associated with fundamental aging processes[16], the metabolic health was evaluated in later life (Fig. 2a). Early-life exercise showed no significant effects on food intake and voluntary physical activity in adulthood in both male and female mice (Fig. 2b–d). Body composition analyses by nuclear magnetic resonance (NMR) revealed that early-life exercise increased lean mass and decreased fat mass in aged male and female mice (24-month-old), while there were no substantial differences in body composition at the age of 14 months in both sexes (Fig. 2e, f). Although early-life exercise decreased total fat mass in aged mice, it increased the mass of brown adipose tissue (BAT) in aged male mice (24-month-old) and subcutaneous white adipose tissue (sWAT) in aged female mice (25-month-old) (Supplementary Fig. 2b, c). In addition, early-life exercise had no effects on circulating lipids but decreased the mass of epididymal white adipose tissue (eWAT) in aged male mice (Supplementary Fig. 2d, e), indicating a fat reduction and redistribution induced by early-life exercise in aged mice.

Regarding blood glucose disposal, early-life exercise did not show significant effects on fasting blood glucose at ages of 4-34 months in both sexes (Fig. 2g). Similarly, there was no substantial differences in random blood glucose and dynamic blood glucose in response to fasting and refeeding in aged male and female mice (19-month-old) (Supplementary Fig. 2f). Interestingly, early-life exercise decreased the circulating levels of insulin at the age of 22–24 months in both sexes, despite no changes in glucose tolerance and insulin tolerance (Fig. 2h, i), suggesting that early-life exercise attenuated age-associated insulin resistance. In addition, metabolic chamber experiments were conducted with aged mice (24-month-old) to assess their metabolic status, in which mice were allowed free access to food for 24 h, followed by a 24 h food deprivation period. There were no differences between mice with and without early-life exercise in terms of energy expenditure, oxygen consumption, carbon dioxide exhalation,

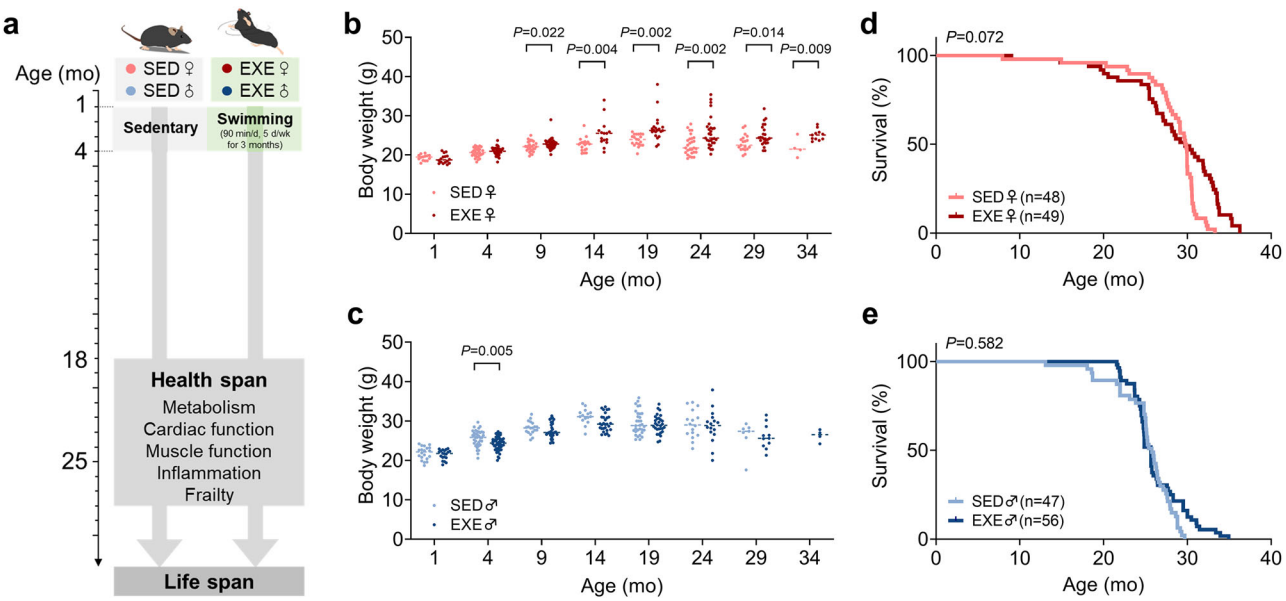

Fig. 1 | Early-life exercise does not extend lifespan in mice. a Experimental timeline. Mice were subjected to sedentary or swimming exercise at 1 to 4 months of age and then reared without exercise training in the rest of the life. **b** and **c** Body weight over the indicated age in female (**b**) and male (**c**) mice. $n = 14, 29, 28, 20, 20, 28, 19$, and 4 for 1, 4, 9, 14, 19, 24, 29, and 34 months of ages for sedentary mice in (**b**) respectively. $n = 16, 40, 38, 15, 20, 29, 24$, and 11 for 1, 4, 9, 14, 19, 24, 29, and 34 months of ages for exercise mice in (**b**) respectively. $n = 20, 37, 19, 15, 32, 16, 7$, and 0 for 1, 4, 9, 14, 19, 24, 29, and 34 months of ages for sedentary mice in (**c**) respectively. $n = 20, 49, 29, 29, 30, 16, 11$ and 4 for 1, 4, 9, 14, 19, 24, 29, and 34 months of ages for exercise mice in (**c**) respectively. **d** and **e** Survival curves of female (**d**) and male (**e**) mice. Data are presented as mean ± SEM. Data are analyzed by two-tailed unpaired Student's t test (**b** and **c**) and the overall survival was tested by Tarone-Ware test (**d** and **e**).

https://doi.org/10.1038/s41467-025-61443-4

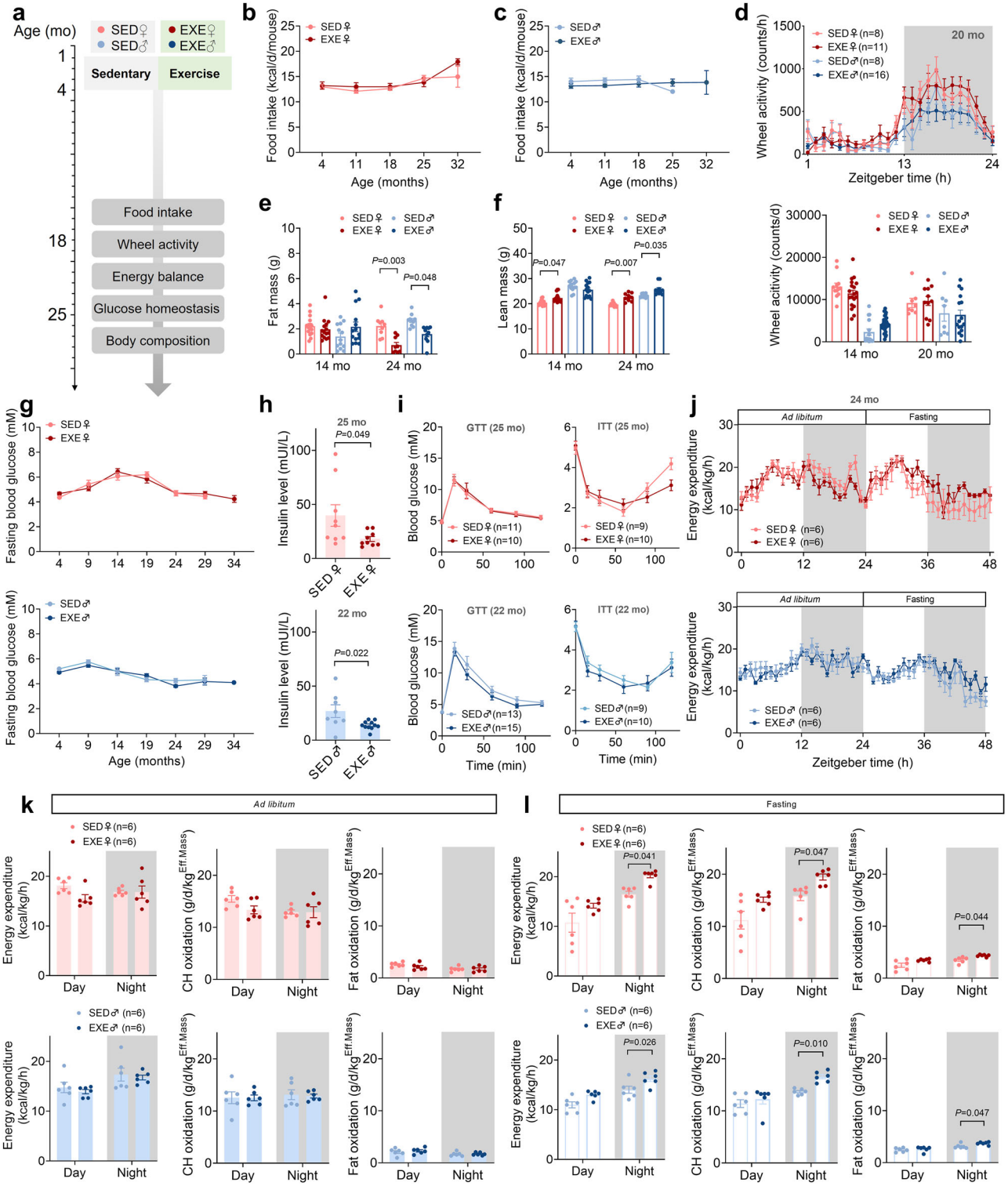

activity, respiratory exchange ratio, carbohydrate oxidation (CHO), and fat oxidation (FO) under feeding condition (Fig. 2j, k, Supplementary Fig. 3). However, after more than 12 h of food deprivation, early-life exercise increased energy expenditure, CHO, and FO level in both aged male and female mice (Fig. 2l). These results suggested that early-life exercise induced metabolic reprogramming in aged mice.

Early-life exercise attenuates cardiovascular aging in aged mice

Aging induces changes in the heart and blood vessels that increase the risks of developing cardiovascular disease. Cardiovascular health was evaluated in adulthood (Fig. 3a). Early-life exercise showed no significant effects on heart rate, blood pressure and cardiac systolic function in both female and male mice at the ages of 5–28 months (Fig. 3b, c and Supplementary Fig. 4a–d). However, it improved the cardiac diastolic function at the age of 19 months (Fig. 3d). Detection of heart weight and cardiac structure revealed no significant changes between mice with and without early-life exercise at the age of 24–25 months. Nevertheless, early-life exercise decreased cardiac fibrosis in aged mice (25-month-old for female mice and 24-month-old for male mice) (Fig. 3e, f). In terms of

Fig. 2 | Early-life exercise increases lean mass and decreases circulating insulin in aged mice. a Experimental timeline. **b** and **c** Food intake over the indicated ages in female (**b**) and male (**c**) mice. $n = 9, 9, 8, 8$, and 4 for 4, 11, 18, 25, and 32 months of ages for sedentary mice in (**b**) respectively. $n = 10, 12, 8, 8$, and 7 for 4, 11, 18, 25, and 32 months of ages for exercise mice in (**b**) respectively. $n = 11, 11, 8, 6$, and 0 for 4, 11, 18, 25, and 32 months of ages for sedentary mice in (**c**) respectively. $n = 11, 11, 9, 8$, and 3 for 4, 11, 18, 25, and 32 months of ages for exercise mice in (**c**) respectively. **d** Voluntary physical activity within one day at 20-month age (up) and voluntary physical activity per day over the indicated ages (down, 14 mo, SED female $n = 12$, EXE female $n = 19$, SED male $n = 15$, EXE male $n = 32$; 20 mo, SED female $n = 8$, EXE female $n = 11$, SED male $n = 8$, EXE male $n = 16$). **e** and **f** Absolute fat mass (**e**) and lean mass (**f**) over the indicated ages (14 mo, SED female $n = 15$, EXE female $n = 15$, SED male $n = 13$, EXE male n = 14; 24 mo, SED female $n = 9$, EXE female $n = 9$, SED male $n = 10$, EXE male $n = 10$). **g**–**i** Fasting blood glucose (**g**, up, $n = 25, 16, 16, 23, 21, 13$, and 0 for 4, 9, 14, 19, 24, 29, and 34 months of ages for sedentary female mice in (**g**) respectively. $n = 25, 20, 15, 19, 19, 19$, and 6 for 4, 9, 14, 19, 24, 29, and 34 months of ages for exercise female mice in (**g**) respectively. down, $n = 45, 18, 15, 16, 13, 3$, and 0 for 4, 9, 14, 19, 24, 29, and 34 months of ages for sedentary male mice in (**g**) respectively. $n = 49, 30, 28, 25, 17, 10$, and 1 for 4, 9, 14, 19, 24, 29, and 34 months of ages for exercise male mice in (**g**) respectively.), serum insulin (**h**, up, $n = 9$ per group; down, SED $n = 8$, EXE $n = 11$), glucose tolerance, and insulin tolerance (**i**) in female and male mice. **j** Energy expenditure normalized to body mass within 48 h under feeding or fasting condition in mice at 24-month age. **k** Quantified exergy expenditure, carbohydrate oxidation, and fat oxidation under feeding condition. **l** Quantified exergy expenditure, carbohydrate oxidation, and fat oxidation under fasting condition. Data are presented as mean ± SEM. Data are analyzed using unpaired, two-tailed Student's *t* test (**h**) and two-way ANOVA with Šídák's multiple comparisons test (**e** and **f, l**).

vascular function, a significant decrease of heart-carotid pulse wave velocity (hcPWV), a biomarker of vascular aging, was observed in both aged male and female mice with early-life exercise (19-month-old), although no significant changes in vascular structure as evidenced by common carotid artery (CCA) diameter and H&E-stained sections of thoracic aortas have been observed (Fig. 3g–j and Supplementary Fig. 4). In addition, examination of vascular function in isolated thoracic aortas revealed that early-life exercise improved endothelial-dependent vascular relaxation without affecting endothelium integrity and smooth muscle cell-dependent relaxation in both aged male and female mice (Fig. 3k–m). Given that cardiac diastolic dysfunction, cardiac fibrosis, upregulated PWV, and endothelial dysfunction are typical biomarkers of cardiovascular aging[17], these results suggested that early-life exercise attenuated cardiovascular aging in aged mice.

Early-life exercise improves musculoskeletal health in aged mice

Skeletal muscle, which accounts for over 40% of body weight, undergoes a decline in both mass and function with aging, leading to dysregulation in mobility, thermo-homeostasis, metabolism, and immunity[18]. The exercise capacity and musculoskeletal health were evaluated in adult mice (Fig. 4a). There were no differences in grip strength and motor coordination between mice with and without early-life exercise at the ages of 5–29 months (Fig. 4b, c). In addition, the differences in endurance exercise capacity were not observed in male and female mice at the age of 18 months (Supplementary Fig. 5a), suggesting that early-life exercise did not change exercise capacity in aged mice. However, tetanic force of tibialis anterior (TA) muscles was increased in 16-month-old male mice with early-life exercise (Fig. 4d). Kyphosis and BMD were measured to assess age-related alterations in bones. Aged mice with early-life exercise had higher kyphosis index (i.e., lower outward curve of the spine) than mice without early-life exercise in both sexes (Fig. 4e). Osteoporosis characterized by bone tissue loss is the primary cause of bone fractures in elderly individuals, particularly among postmenopausal women. We observed that early-life exercise increased BMD merely in aged female mice (Fig. 4e). Detection of muscle mass showed no significant differences induced by early-life exercise in female and male mice at the age of 24 and 25 months (Supplementary Fig. 5a, b). However, morphology analyses revealed that early-life exercise increased the myofiber cross-section area (CSA) in female and male mice at the age of 24 and 25 months (Fig. 4f). Early-life exercise also reduced fibrosis and increased capillary density (capillaries per fiber) in skeletal muscles in aged mice (Fig. 4g, h). Immunofluorescence showed that early-life exercise decreased resident macrophages (CD11b-positive) in skeletal muscles of aged mice (Fig. 4i). Early-life exercise also decreased the contents of Atrogin 1, a marker of muscle atrophy, in skeletal muscles of aged mice (Fig. 4j). Furthermore, we assessed the mRNA expression levels of major skeletal muscle-derived exerkines in aged male mice (24-month-old) and found that nearly half of the detected exerkines were upregulated in expression in mice subjected to early-life exercise, including *Il6*, *Vegfd*, *Vegfa*, and *Cxcl1* (Fig. 4k). These results suggested that early-life exercise improved bone and muscle strength in aged mice.

Early-life exercise decreases inflammation and frailty in aged mice

Inflammaging, or age-related multi-organ chronic inflammation, is a fundamental hallmark of aging[19]. We observed an elevated fraction of granulocytes among circulating leukocytes, which serves as an indicator of ongoing inflammation, in aged mice; nevertheless, early-life exercise decreased the fraction of granulocytes in aged female and male mice (Fig. 5a, b). The percentage of lymphocytes (Lym%) among circulating leukocytes declined with aging and early-life exercise attenuated this process in aged female and male mice (Fig. 5c). No differences were observed in circulating platelet count, hemoglobin content, red blood cell count, and white blood cell count between mice with and without early-life exercise in both sexes at the ages of 4 months and 26 months (Supplementary Fig. 6a–d). C-reactive protein (CRP), not only an inflammatory biomarker but also an important risk factor for aging-related diseases, was not changed by early-life exercise in aged male mice (Supplementary Fig. 6e). Serum cytokines were also detected by a cytokine/chemokine array in aged male and female mice. The results showed that some of the cytokines/chemokines were decreased in aged mice with early-life exercise (Fig. 5d). Furthermore, reduced inflammaging was also evidenced by the lower number of histologically discernable perivascular inflammatory infiltrates in livers (Fig. 5e) and alveolar inflammatory infiltrates in the lungs of aged mice with early-life exercise (Supplementary Fig. 6g). CD11b-positive cells, representing macrophages, were also reduced in livers and lungs from aged mice with early-life exercise (Supplementary Fig. 6h, i). These results suggested that early-life exercise reduces inflammation in aging.

Mice become increasingly frail with age, and their frailty was assessed at 24–28 months old (Fig. 5a). Notably, early-life exercise resulted in observational alleviation in alopecia and fur color loss (change in fur color from black to gray or brown) in aged mice (Fig. 5f). The total frailty index score, an average of 31 frailty phenotypes, showed an increase corresponding to aging phenotypes. Both male and female mice with early-life exercise exhibited lower frailty index score in aged mice, indicating that early-life exercise attenuates age-related phenotypes (Fig. 5g). Further analysis of the frailty index showed variations in the effects of early-life exercise on frailty phenotypes between sexes, both in terms of degree and incidence (Fig. 5h, i and Supplementary Fig. 7). For example, early-life exercise decreased the degree of kyphosis frailty, coat condition, loos of fur color, and alopecia in both sexes, but only decreased the degree of cataracts in female mice and loss of whiskers in male mice

https://doi.org/10.1038/s41467-025-61443-4

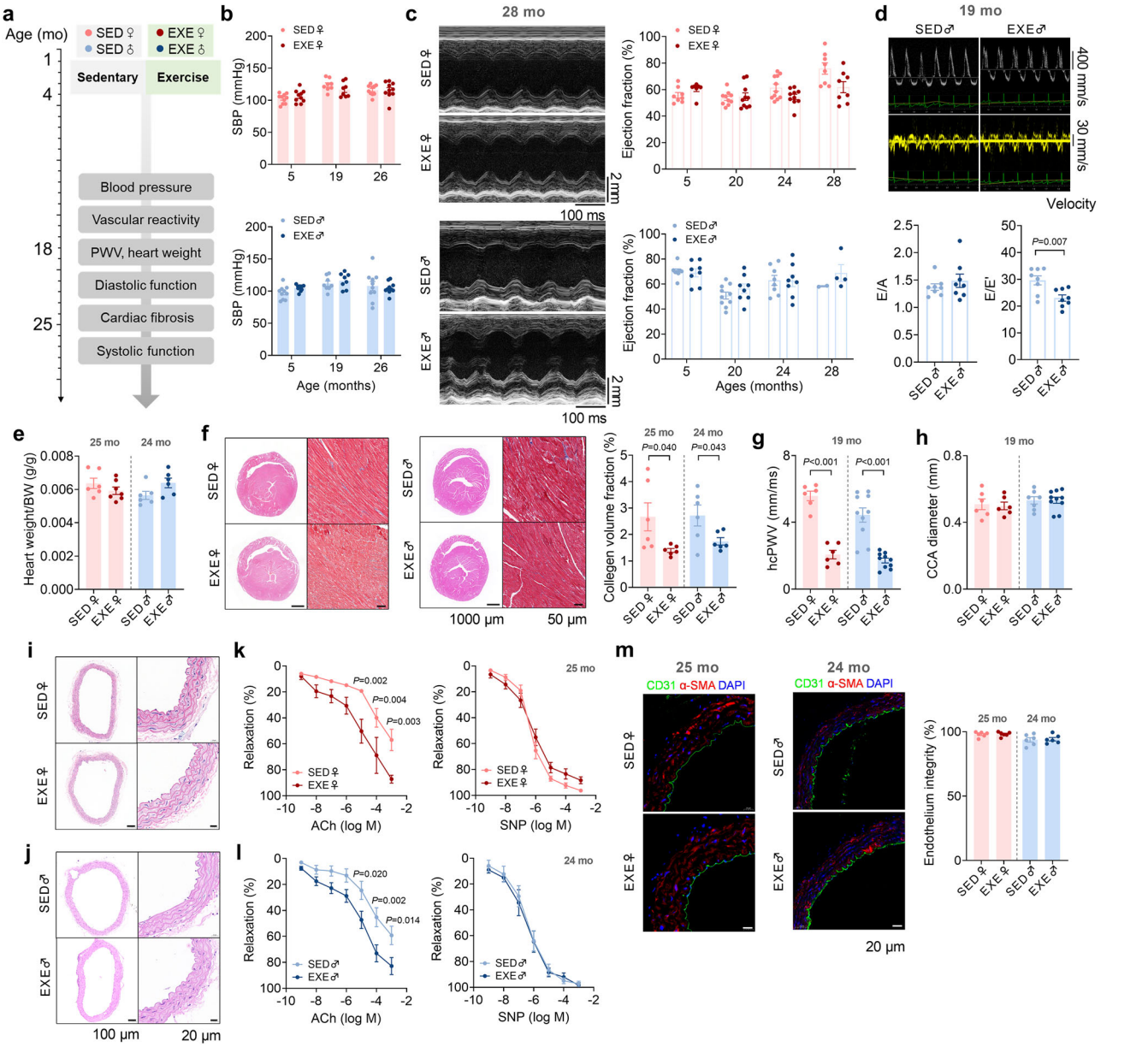

Fig. 3 | Early-life exercise attenuates cardiovascular aging in aged mice. **a** Experimental timeline. **b** Systolic blood pressure (SBP) over the indicated ages in female and male mice (up, n = 10, 8 and 10 for 5, 19 and 26 months of ages for sedentary female mice in (**b**) respectively. $n = 10$, 8 and 10 for 5, 19 and 26 months of ages for exercise female mice in (**b**) respectively. down, $n = 10$, 8 and 10 for 5, 19 and 26 months of ages for sedentary male mice in (**b**) respectively. $n = 10$, 8, and 10 for 5, 19, and 26 months of ages for exercise male mice in (**b**) respectively). **c** Cardiac systolic function over the indicated ages in female and male mice (up, n = 8, 10, 11, and 8 for 5, 20, 24, and 28 months of ages for sedentary female mice in (**c**) respectively. $n = 7$, 10, 10, and 8 for 5, 20, 24, and 28 months of ages for exercise female mice in (**c**) respectively. down, $n = 8$, 10, 8, and 2 for 5, 20, 24, and 28 months of ages for sedentary male mice in (**c**) respectively. $n = 8$, 8, 8, and 4 for 5, 20, 24, and 28 months of ages for exercise male mice in (**c**) respectively). **d** Cardiac diastolic function in male mice at the age of 19 months ($n = 8$). **e** Heart weight/body weight over the indicated age (SED female $n = 6$, EXE female $n = 7$, SED male $n = 6$, EXE male $n = 6$). **f** Cardiac fibrosis stained by Masson at 25-month age for female mice ($n = 6$) and 24-month age for male mice ($n = 6$). **g** Heart-carotid pulse wave velocity (hcPWV) in mice at 19-month age (female, $n = 6$ per group; male, $n = 10$ per group). **h** Common carotid artery (CCA) diameter in mice at 19-month age (SED female $n = 6$, EXE female $n = 6$, SED male $n = 7$, EXE male $n = 10$). **i** and **j** H&E-stained thoracic aorta sections in female (25-month-old) (i) and male (24-month-old) (j) mice. **k** and **l** Acetylcholine (ACh)- and sodium nitroprusside (SNP)-induced vasodilation in isolated thoracic aortas in female (**k**, SED $n = 7$, EXE $n = 6$) and male (**l**, $n = 7$ per group) mice. **m** Immunofluorescence of CD31 and α-smooth muscle actin (α-SMA) in thoracic aorta sections in female and male mice ($n = 6$). Endothelium integrity was quantified. Data are presented as mean ± SEM. Data are analyzed using unpaired, two-tailed Student's t test (**d**, **f** and **g**) and two-way ANOVA with Šídák's multiple comparisons test (**k** and **l**).

(Fig. 5h). Interestingly, early-life exercise tended to decrease the incidence of age-related phenotypes, including alopecia, loss of fur color, loss of whiskers, coat condition, and kyphosis, only in male mice (Fig. 5i). A detailed pathological examination of dead mice revealed that early-life exercise had no obvious effects on tumor burden at death, which is the leading cause of death in both sexes in C57BL/6J mice (Fig. 5j). According to two recently developed indexes for quantifying healthspan[20], Frailty-Adjusted Mouse Years and Gauging Robust Aging when Increasing Lifespan, early-life exercise increased the healthspan of mice by 0.20–0.51 years (Fig. 5k). These results suggested that early-life exercise mitigates age-associated frailty.

https://doi.org/10.1038/s41467-025-61443-4

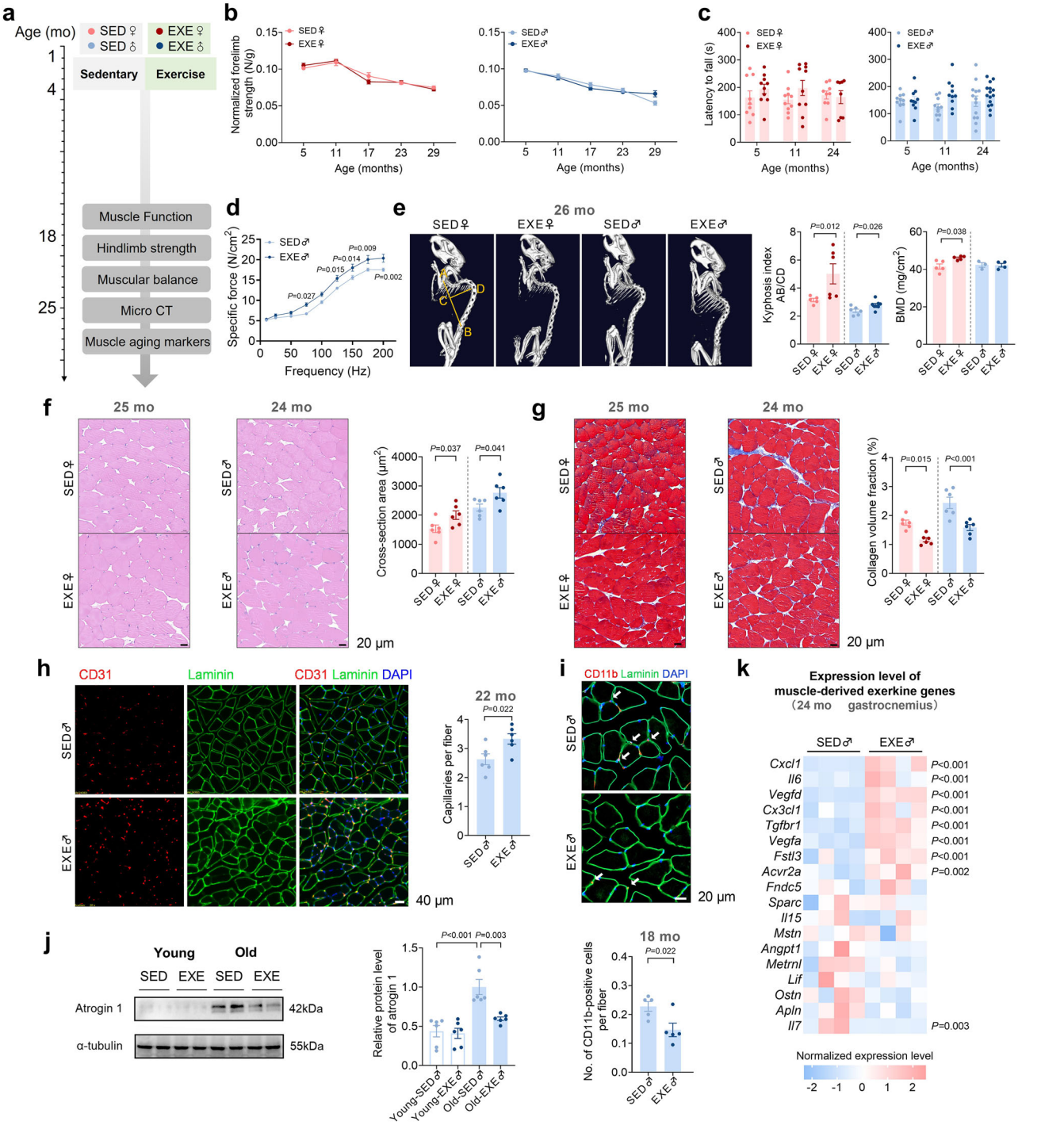

Fig. 4 | Early-life exercise improves musculoskeletal health in aging. **a** Experimental timeline. **b** Grip strength over the indicated ages in female and male mice (left, $n = 25$, 15, 8, 22, and 19 for 5, 11, 17, 23, and 29 months of ages for sedentary female mice in (**b**) respectively. $n = 25$, 15, 8, 25, and 24 for 5, 11, 17, 23, and 29 months of ages for exercise female mice in (**b**) respectively. right, $n = 25$, 15, 8, 25, and 3 for 5, 11, 17, 23, and 29 months of ages for sedentary male mice in (**b**) respectively. $n = 25$, 15, 8, 25, and 7 for 5, 11, 17, 23, and 29 months of ages for exercise male mice in (**b**) respectively.). **c** Motor coordination over the indicated ages (left, $n = 9$, 10, and 9 for 5, 11, and 24 months of ages for sedentary female mice in (**c**) respectively. $n = 10$, 10, and 8 for 5, 11, and 24 months of ages for exercise female mice in (**c**) respectively. right, $n = 10$, 10, and 13 for 5, 11, and 24 months of ages for sedentary male mice in (**c**) respectively. $n = 10$, 10 and 15 for 5, 11, and 24 months of ages for exercise male mice in (**c**) respectively). **d** Tetanic force-frequency relationships of tibialis anterior muscles from male mice at the ages of 16 months ($n = 6$). **e** Kyphosis index (SED female $n = 5$, EXE female $n = 6$, SED male $n = 6$, EXE male $n = 8$) and bone mineral density (BMD) in aged mice (SED female $n = 5$, EXE female $n = 5$, SED male $n = 3$, EXE male $n = 4$). **f** H&E-stained gastrocnemius muscle sections and quantified myofiber cross-section area (CSA) at the indicated age ($n = 6$). **g** Masson-stained gastrocnemius muscle sections and quantified fibrosis ($n = 6$). The collagen volume fraction (%) was calculated as the ratio of collagen volume to fiber volume. **h** CD31 immunofluorescence in gastrocnemius muscle sections from aged male mice ($n = 6$). **i** CD11b immunofluorescences in the gastrocnemius muscle from aged mice ($n = 5$). Arrows indicated CD11b-positive cells. **j** Atrogin 1 contents in gastrocnemius muscles from young and aged mice (Young, 4 mo; old, 18 mo; $n = 6$). **k** Expressions of genes encoding exerkines in gastrocnemius muscles from aged male mice. $n = 4$. Data are presented as mean ± SEM. Data are analyzed using unpaired, two-tailed Student's t test (**e**–**i**, **k**), one-way ANOVA with Tukey's multiple comparisons test (**j**) and two-way ANOVA with Šídák's multiple comparisons test (**d**).

https://doi.org/10.1038/s41467-025-61443-4

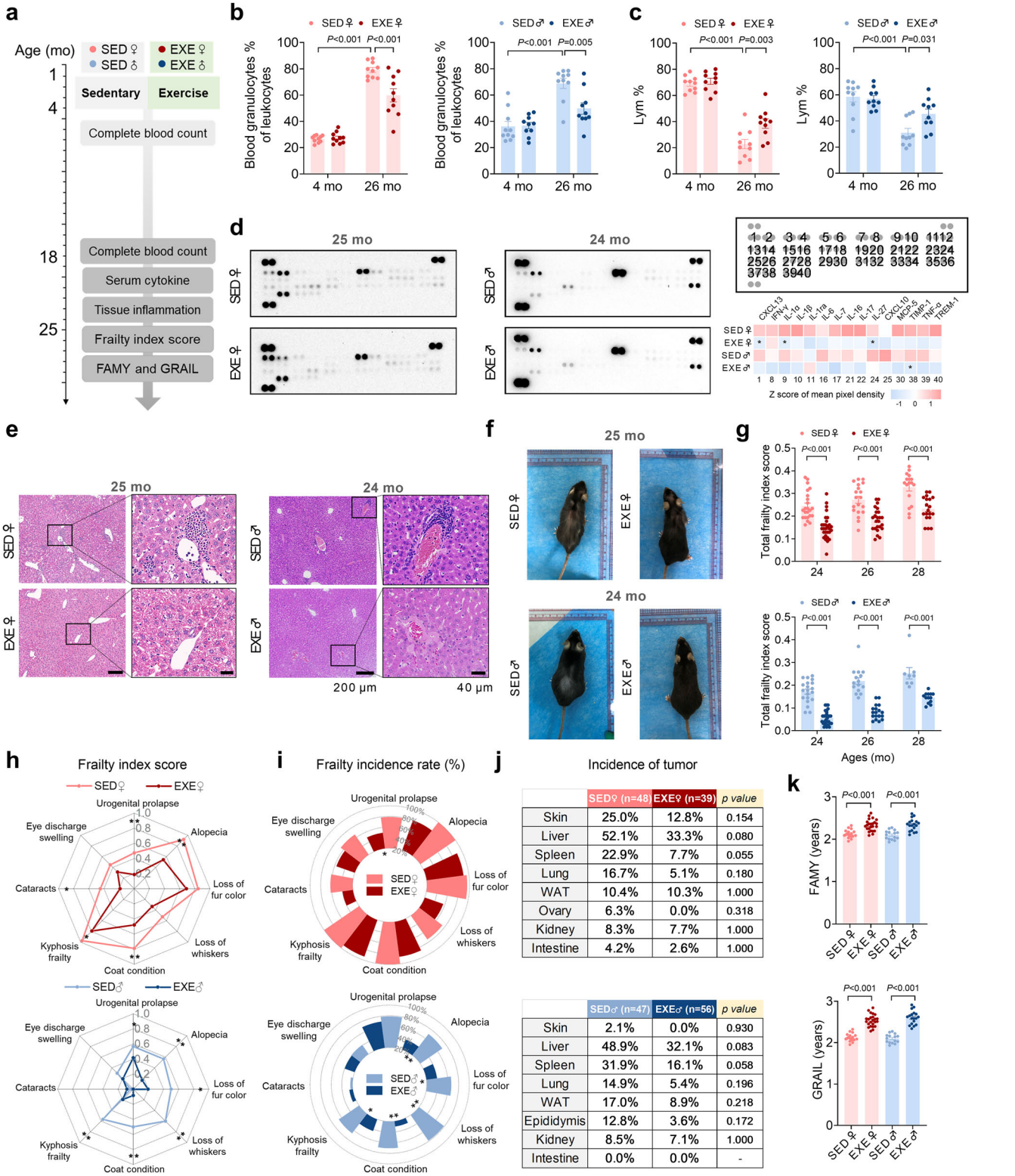

	SED♀ (n=48)	EXE♀ (n=39)	*p* value
Skin	25.0%	12.8%	0.154
Liver	52.1%	33.3%	0.080
Spleen	22.9%	7.7%	0.055
Lung	16.7%	5.1%	0.180
WAT	10.4%	10.3%	1.000
Ovary	6.3%	0.0%	0.318
Kidney	8.3%	7.7%	1.000
Intestine	4.2%	2.6%	1.000

	SED♂ (n=47)	EXE♂ (n=56)	*p* value
Skin	2.1%	0.0%	0.930
Liver	48.9%	32.1%	0.083
Spleen	31.9%	16.1%	0.058
Lung	14.9%	5.4%	0.196
WAT	17.0%	8.9%	0.218
Epididymis	12.8%	3.6%	0.172
Kidney	8.5%	7.1%	1.000
Intestine	0.0%	0.0%	-

mRNA sequencing reveals an attenuated aging by early-life exercise

To gain molecular insights into the effects of early-life exercise on promoting healthy aging, we performed transcriptional profiling of the liver, gastrocnemius muscle, heart, and eWAT from male mice at different ages (4, 18, and 24 months). Principal-component analysis (PCA) showed that while the transcriptome of SED and EXE mice at 4-month age substantially overlapped, it diverged as the mice aged, indicating distinct aging processes at molecular level between mice with and without early-life exercise (Fig. 6a). The number of differentially expressed genes (DEGs) was also increased with age (Fig. 6b). Aging DEGs (Old-SED vs. Young-SED) and Exercise DEGs (Old-EXE vs. Old-SED) were initially analyzed for further identifying anti-aging effects of early-life exercise. Genes that changed in opposite directions between Aging DEGs and Exercise DEGs were categorized as Rev-aging DEGs, while Pro-aging DEGs referred to genes that changed in the same manner (Fig. 6c). The validation of this methodology was also performed, and the results showed that Aging DEGs mainly enriched in

Fig. 5 | Early-life exercise decreases frailty and inflammation in aging. **a** Experimental timeline. **b** Fraction of granulocytes among circulating leukocytes in young and aged mice ($n = 10$). **c** Percentage of lymphocytes among circulating leukocytes in young and aged mice ($n = 10$). **d** Cytokine array of serum from old male and female mice ($n = 3$, $^*P < 0.05$). Typical images and heatmap of quantified serum cytokines were shown. **e** Representative images of H&E-stained liver sections from aged mice ($n = 6$). Perivascular and perinecrotic immune cell infiltrates were enlarged in boxed areas. **f** Typical mice photos at 24-25 months old. **g** Frailty indexes over the indicated ages (up, $n = 23$, 19, and 17 for 24, 26, and 28 months of ages for sedentary female mice in (**g**), respectively. $n = 29$, 24, and 19 for 24, 26, and 28 months of ages for exercise female mice in (**g**), respectively. down, $n = 20$, 15, and 8 for 24, 26, and 28 months of ages for sedentary male mice in (**g**), respectively. n=29, 18, and 13 for 24, 26, and 28 months of age for exercise male mice in (**g**), respectively). **h** Average frailty index score in different types of frailty phenotypes in mice at the age of 26 months (SED female $n = 19$, EXE female $n = 24$, SED male $n = 15$, EXE male $n = 18$; $^*P < 0.05$, $^{**}P < 0.01$). **i** Incidence of frailty phenotypes in mice at the age of 26 months (SED female $n = 19$, EXE female $n = 24$, SED male $n = 15$, EXE male $n = 18$; $^*P < 0.05$, $^{**}P < 0.01$). **j** Tumor burden in mice that died of natural causes. Presence of apparent neoplastic lesions at the time of sacrifice was recorded. **k** Early-life exercise extended the healthspan of mice as evaluated by FAMY and GRAIL (SED female $n = 18$, EXE female $n = 24$, SED male $n = 15$, EXE male $n = 18$). Data are presented as mean ± SEM. Data are analyzed using unpaired, two-tailed Student's test (**d** and **h**), Chi-square test (**i** and **j**), one-way ANOVA with Tukey's multiple comparisons test (**k**) and two-way ANOVA with Šídák's multiple comparisons test (b, c and g).

aging related genes and pathways (Supplementary Fig. 8f, g). Rev-aging DEGs displayed anti-aging effects of early-life exercise (Supplementary Fig. 8h). The number and ratio of Rev-aging DEGs were higher than Pro-aging DEGs in the liver, muscle, and heart, especially at 18 months of age (Fig. 6d and Supplementary Fig. 8a). Functionally, enrichment analysis showed that the upregulated Rev-aging DEGs converged into energy metabolism and cell morphogenesis related gene ontology (GO) pathways, including fatty acid oxidation and oxidative phosphorylation (Fig. 6e). In contrast, the downregulated Rev-aging DEGs across tissue types were enriched in GO terms associated with inflammation, stress, cell death, DNA damage, and aging (Fig. 6e). In addition, fold changes of DEGs among multiple tissues in mice with early-life exercise (Old-EXE vs. Young-EXE) were decreased as compared to the fold changes of DEGs in sedentary mice (Old-SED vs. Young-SED) (Fig. 6f), indicating that early-life exercise attenuated age-related changes. If there were no rescue by early-life exercise, the data points would fall on the unity line (slope = 1). The anti-aging effects of early-life exercise were further confirmed by senescence-associated β-galactosidase (SA-β-gal) staining and Western blots. SA-β-gal activity in the liver was decreased by early-life exercise in both male and female mice at 18 months of age (Fig. 6g). Consistently, levels of hepatic and muscular p16 and p21 were down-regulated by early-life exercise in 18-month-old mice (Fig. 6h). These results suggested that early-life exercise attenuates aging at the molecular level, especially in the muscle, heart, and liver.

Early-life exercise improves fatty acid utilization in skeletal muscles in aged mice

Considering the beneficial effects of early-life exercise on systemic metabolism in aged mice and the significant role of metabolic disorder in aging process, we investigated the molecular-level metabolic regulation induced by early-life exercise. Kyoto Encyclopedia of Genes and Genomes (KEGG) enrichment analyses of DEGs in liver, skeletal muscle, heart, and eWAT revealed that early-life exercise tended to affect lipid metabolism more significantly, with enrichment in pathways, such as peroxisome proliferator-activated receptor (PPAR) signaling and fatty acid metabolism (Fig. 7a and Supplementary Fig. 9). These changes were most prominent in skeletal muscles and hearts (Fig. 7a). Gene set enrichment analysis (GSEA) showed that genes involved in lipid and fatty acid metabolic processes were upregulated in skeletal muscles but not in the liver of aged mice with early-life exercise (Fig. 7b). Specifically, early-life exercise upregulated the expression of almost all genes coding proteins in the fatty acid metabolism pathway, including fatty acid transport, lipolysis, fatty acid oxidation, TCA cycle, and oxidative phosphorylation, and these changes were not observed in the liver (Fig. 7c). Protein contents of several key enzymes linked to fatty acid metabolism were analyzed in the muscles and livers from young (4-month-old) and aged (18-month-old) mice. Carnitine palmitoyl transferase 1B (CPT1B, translocating fatty acids across the mitochondrial membranes), CD36 (translocating fatty acids into cells) and acyl-Coenzyme A dehydrogenase-long chain (ACADL, catalyzing the initial step of mitochondrial β-oxidation) contents were increased, and fatty acid synthase (FASN) (FASN, catalyzing the synthesis of long-chain fatty acids) content was reduced in muscles of aged mice with early-life exercise (Fig. 7d). While in the liver, FASN protein was upregulated and CPT1A and CD36 were downregulated by early-life exercise in aged mice (Fig. 7d). Detection of mitochondrial function-related proteins in skeletal muscles revealed no differences between mice with and without early-life exercise at the age of 18 months (Fig. 7d and Supplementary Fig. 9d). Oxygen respiration analysis was performed to detect the fatty acid oxidation and CHO directly in permeabilized muscle fibers from male mice at the age of 16 months. The results showed that early-life exercise increased both the resting and the maximal OXPHOS capacity of fatty acid oxidation without significant effects on CHO of muscle fibers (Fig. 7e, f). Additionally, mRNA expression level of genes involved in fatty acid metabolism were significantly increased in eWAT in aged mice with early-life exercise (Supplementary Fig. 9g, h). mTOR signaling generally dampens with exercise and closely related to longevity and fatty acid oxidation, which were enriched in skeletal muscles (Fig. 7a). However, no changes in mTOR signaling pathway were observed in skeletal muscles from aged mice with early-life exercise (Supplementary Fig. 9e, f). These results indicated that early-life exercise improves fatty acid utilization in skeletal muscles in aged mice, which may contribute to the anti-aging effect of this intervention.

Discussion

Physical inactivity is a growing public health concern worldwide. This trend is particularly alarming among youth populations, who are increasingly leading sedentary lifestyles due to factors, such as smartphone addiction, screen time, excessive homework and reduced physical activity opportunities. The lifestyle in this population can impact the risk of adverse health outcomes and healthcare costs in adulthood from a life course perspective. However, the significance of early-life exercise has not received sufficient attention. In this study, we investigated the effects of early-life exercise alone on overall health and healthspan in mice. Our findings provided evidence that early-life exercise did not extend lifespan, but significantly extended healthspan in both male and female mice, as evidenced by improved metabolism, cardiovascular function, muscle strength, and mitigated inflammation and frailty in aged mice (Fig. 8). These findings provide valuable insights into understanding the long-term effects of exercise and underscore the importance of regular physical activity from an early age to optimize health outcomes over lifetime and promote healthy aging.

Physical inactivity represents a major independent risk factor for mortality, with physically active persons exhibiting a 20–35% reduction in the risk of all-cause mortality[21,22], and considering that a 40% lower mortality rate corresponds to an approximately 5-year higher life expectancy[23], it is anticipated that physically active individuals may gain around 3.5–4.0 additional years of life. Previous studies have

https://doi.org/10.1038/s41467-025-61443-4

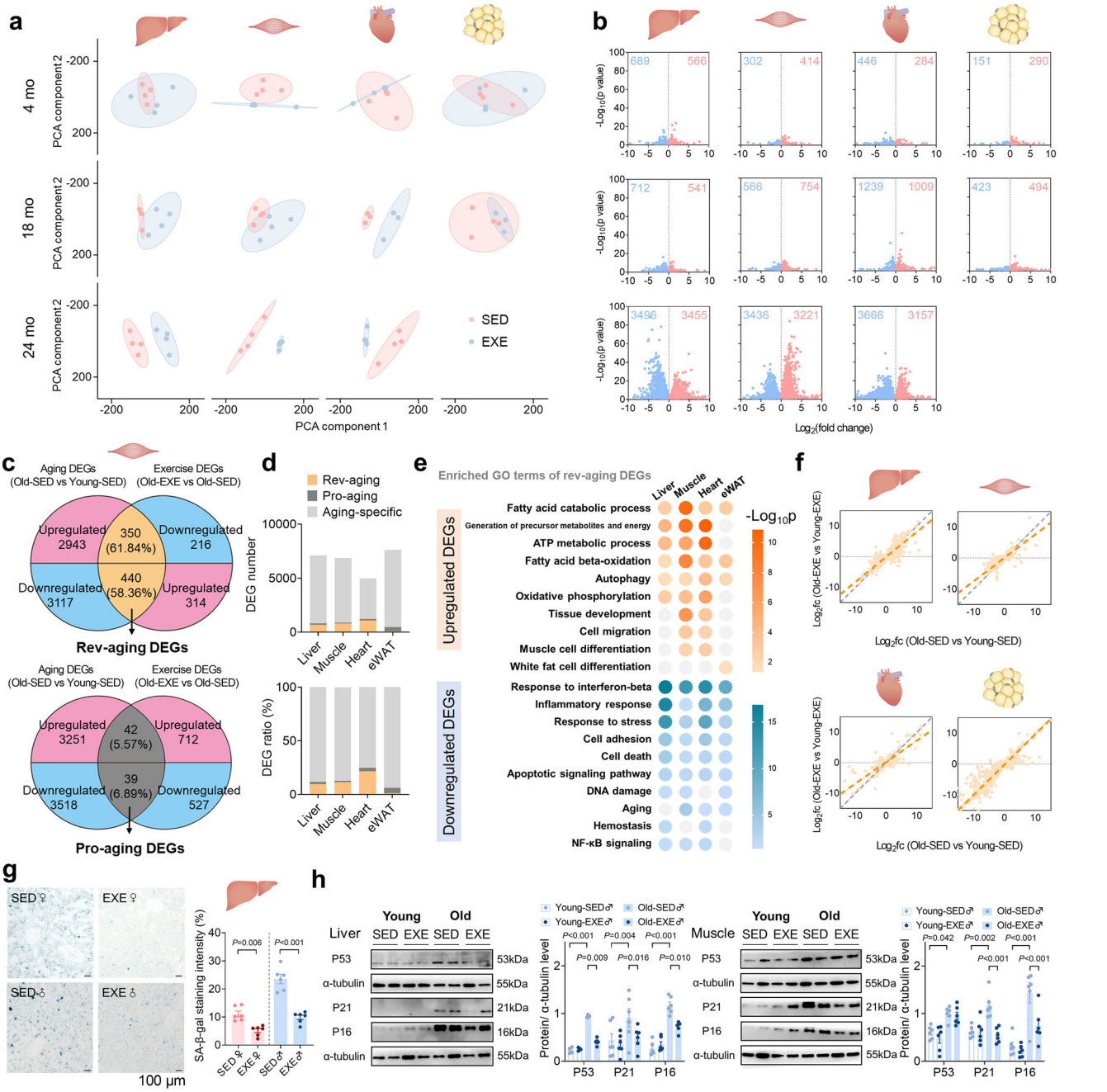

Fig. 6 | mRNA sequencing reveals an attenuated aging by early-life exercise. **a** PCA analyses of the transcriptome data of the liver, gastrocnemius muscle, heart, and eWAT from 4-month-old, 18-month-old, and 24-month-old male mice. $n = 3$ for heart of 18 mo SED and EXE, others $n = 4$. **b** Volcano plot for differently expressed genes (DEGs) (EXE vs. SED) in different tissues from mice over the indicated ages. Red denotes upregulated genes; blue denotes downregulated genes. **c** Venn diagrams showing the overlapped DEGs between Aging DEGs and Exercise DEGs in skeletal muscles based on RNA-seq data from 4 mo (Young) and 18 mo (Old) mice. Aging DEGs is defined as Old-SED vs. Young-SED and Exercise DEGs is defined as Old-EXE vs. Old-SED. If a DEG was increased in aging, but decreased between early-life exercise group, it belongs to "Rev-aging DEGs" group. If changed in the same manner, the gene belongs to "Pro-aging DEGs" group. **d** Bar plots showing the ratio (up) and number (down) of Rev-aging, Pro-aging and Aging-specific DEGs in different tissues based on RNA-seq data from 4 and 18 mo mice. Aging DEGs excluding Rev-aging and Pro-aging DEGs are defined as Aging-specific DEGs. **e** Heatmaps showing the enriched GO pathways for upregulated and downregulated Rev-aging DEGs by early-life exercise among multiple tissues based on RNA-seq data from 4 and 18 mo mice. **f** Spearman correlation plots comparing changes in DEGs expression between SED and EXE groups based on RNA-seq data from 4 mo and 18 mo mice. **g** Senescence-associated beta galactosidase staining analysis (SA-β-gal) in liver sections from aged male (18 mo) and female (18 mo) mice ($n = 6$). **h** Immunoblotting analyses of senescence biomarkers (p53, p21, and p16) in liver and muscle from young (4 mo) and old (18 mo) mice ($n = 6$). Data are presented as mean ± SEM. Data are analyzed using hypergeometric test (**e**), one-way ANOVA with Tukey's multiple comparisons test (**g**) and two-way ANOVA with Šídák's multiple comparisons test (**h**).

reported a higher life expectancy in physically active subjects, ranging from 0.43 to 6.9 additional years[24]. However, direct evidence regarding the effects of physical activity or exercise on lifespan is limited. Animal studies show inconsistent results. It is reported that life-long spontaneous aerobic exercise did not prolong longevity in mice, but extended healthspan as observed in other studies[25]. It is also reported that treadmill training for 50 weeks extended lifespan in rats[26]. The causal relationship between exercise and lifespan needs to be further

https://doi.org/10.1038/s41467-025-61443-4

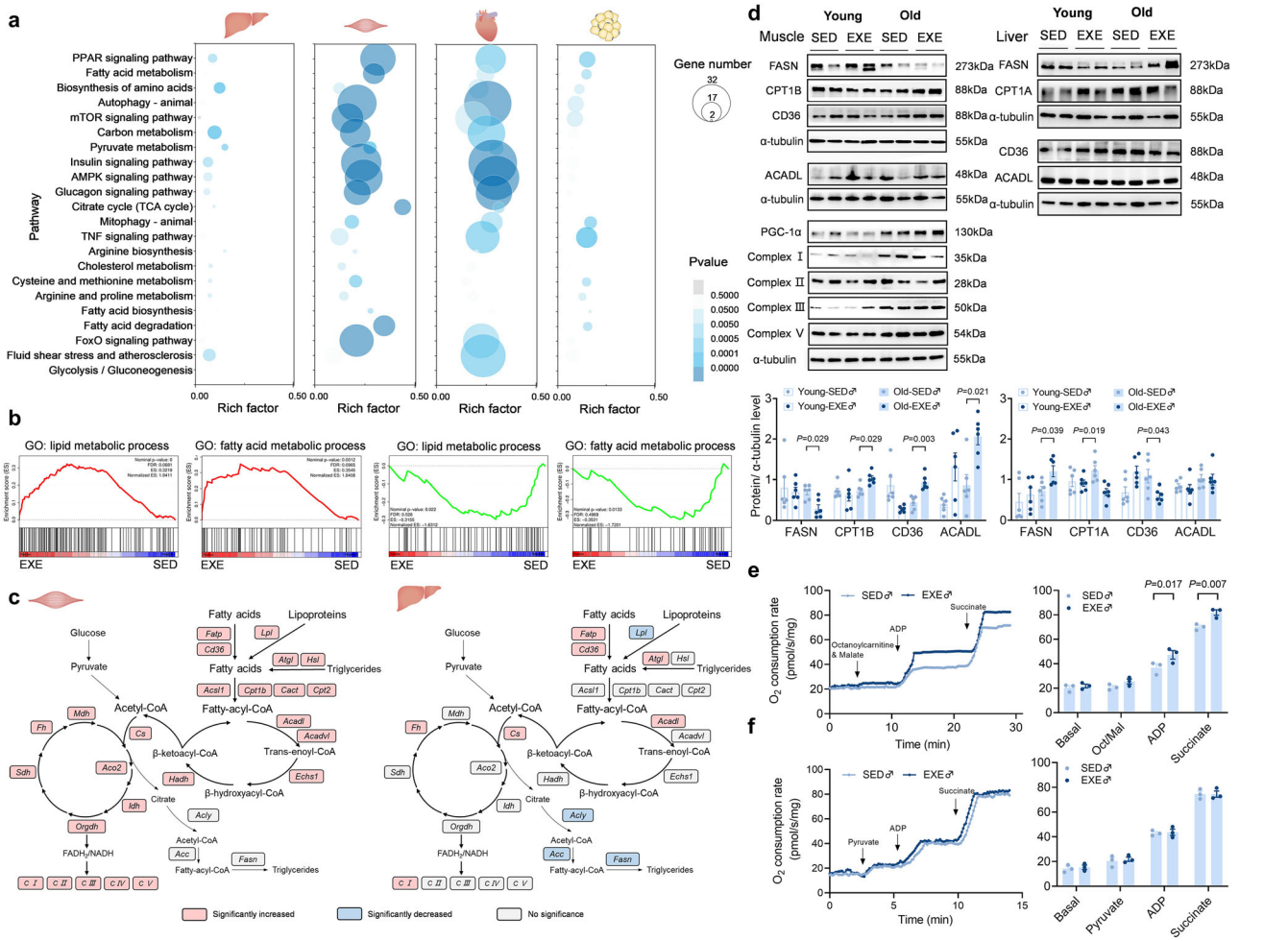

Fig. 7 | Early-life exercise improves fatty acid utilization in skeletal muscles in aging. a KEGG enrichment analysis identifying the effects of early-life exercise on metabolic pathways in aged mice (18 mo). Size and color of dot indicate number and significance of genes mapped to specific pathways. Significant ($p < 0.05$) pathways are shown with color. Rich factor refers to the ratio of DEG numbers annotated in this pathway term to all gene numbers annotated in this pathway term. **b** Gene set enrichment analysis showing relative gene expression involved in lipid and fatty acid metabolic processes in muscle (left) and liver (right) tissues from aged mice based on 18 mo RNA-seq data. **c** Pathway diagrams involving glycolysis, fatty acid transport, lipolysis, lipogenesis, fatty acid oxidation, TCA cycle and oxidative phosphorylation, showing gene expression changes induced by early-life exercise in muscles and livers from aged mice (18 mo). **d** Immunoblotting analyses of lipid metabolic proteins and mitochondrial function biomarkers in muscles and livers from young (4 mo) and old (18 mo) male mice ($n = 6$). FASN, fatty acid synthase; CPT1A/B, carnitine palmitoyltransferase 1A/B; ACADL, acyl-Coenzyme A dehydrogenase, long chain; PGC-1α, PPARγ coactivator-1α. **e** Representative records of O_2 consumption rate and quantified respiration of permeabilized muscle fibers from male mice (16 mo) using octanoylcarntine and malate as substrates. Adenosine diphosphate (ADP) was added to stimulate fatty acid oxidation respiration. To achieve maximal physiological oxidative phosphorylation capacity, succinate was added ($n = 3$). **f** Representative records of O_2 consumption rate and quantified respiration of permeabilized muscle fibers from male mice (16 mo) using pyruvate as substrates ($n = 3$). Data are presented as mean ± SEM. Data are analyzed using hypergeometric test (**a**), permutation test (**b**) and two-way ANOVA with Šídák's multiple comparisons test (**d** and **e**).

examined. Here, we observed that early-life exercise for 3 months only increased the maximum lifespan without affecting the medium lifespan and overall survival in both male and female mice, although early-life exercise induced a healthier phenotype in aged mice.

Previous studies often focus on the transient beneficial effects afforded by exercise, while recent studies have revealed a long-term beneficial effect of exercise through epigenetic modulation[27,28]. For example, it is reported that physical activity in youth was associated with lower rates of occurrence of chronic diseases in adulthood, and higher physical activity in childhood is associated with increased aerobic fitness and BMD, and decreased risks for developing metabolic diseases later in life[11–13]. These advances suggest that early-life exercise benefits human health in adulthood. In addition, maternal or paternal exercise prevents age-associated and high-fat diet-induced metabolic dysfunction in offspring[29,30]. Here, we found that early-life exercise promotes healthy aging without inducing significant increase in physical activity in adulthood. Early-life exercise increased lean mass, decreased fat mass and serum insulin, elevated energy expenditure under fasting condition, improved cardiac diastolic function, attenuated vascular aging, enhanced muscle strength, decreased systemic inflammation, and attenuated frailty in aged mice. The anti-aging effects of early-life exercise were further validated by multiple-tissue transcriptome analyses. Early-life exercise increased the expression of anti-aging genes in aged mice, especially at age of 18 months. It is reported that exercise induces extensive epigenetic modulation[31,32], which may contribute to the long-term effect of early-life exercise. Further studies are warranted to explore the underling mechanisms.

Aging and metabolism share an intricate relationship, where many age-related metabolic changes, including shifts in body composition, dysregulated nutrient-sensing, and mitochondrial dysfunction, are fundamentally associated with aging processes[19,33]. Aging is often associated with gain in body fat, reduction in lean mass, insulin

https://doi.org/10.1038/s41467-025-61443-4

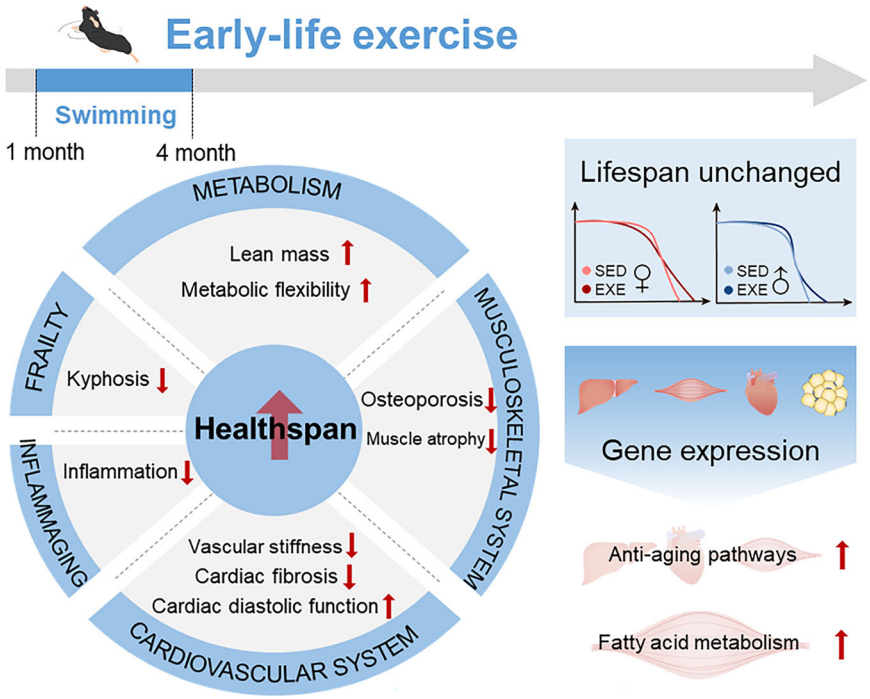

Fig. 8 | Schematic depicting long-term effects of early-life exercise on lifespan and healthspan. Early-life exercise exerts enduring long-term health benefits, improving healthspan, but not lifespan, in both male and female mice. Enhanced fatty acid metabolism in skeletal muscles is identified as a major feature in aged mice that underwent early-life exercise.

resistance, decreased energy production and expenditure, impaired fatty acid oxidation, and compromised metabolic flexibility and elasticity[17,34,35]. Here, we provided evidence that early-life exercise increased lean mass, decreased fat mass, lowered circulating insulin, improved fatty acid metabolism, and increased metabolites utilization and energy expenditure in response to fasting in aged mice, indicating an improvement in metabolic health. Specifically, transcriptome analyses revealed that the enhanced fatty acid metabolism in skeletal muscles is one of the most significant changes induced by early-life exercise in aging. During aging processes, the circulating levels of most lipid subclasses increase[36], and the capacity of fatty acid oxidation is decreased in multiple organs[19,37,38]. Conversely, elevated fatty acid oxidation is identified as the most significant metabolic feature in long-lived individuals[39], and improvement in fatty acid metabolism tends to promote healthy aging and prolong lifespan[40]. The altered fatty acid metabolism in aging is accompanied with lipid accumulation in non-adipose tissue, inflammation, insulin resistance, oxidative stress, chromatin modifications, and energy deficiency which accelerate cellular senescence[41]. Thus, it is suggestive that enhanced fatty acid metabolism in skeletal muscles is a key mechanism underlying the early-life exercise-afforded benefits in promotion of healthy aging. These findings align with previous studies linking metabolic adaptations to exercise and highlight the importance of metabolic health in promoting healthy aging. As we only analyzed gastrocnemius muscle in the study, more experiments are warranted to detect the changes of different muscles in response to early-life exercise to get a more comprehensive understanding.

Sex disparities in aging and lifespan are notable due to factors such as sex hormones, genome, risk exposure, lifestyle, and others. In general, females exhibit longer lifespans but they may experience greater morbidity particularly in later life, although evidence in mice is inconsistent[42]. One of the most obvious features of sex differences in aging is that age-related decline in BMD is more pronounced in women than in men[43]. Females also experience greater age-related cardiovascular phenotypes, including wall thickening, myocardial stiffening, cardiac diastolic dysfunction, earlier onset of coronary microvascular dysfunction, and arterial stiffness[44]. Exercise-induced adaptations also exhibit sex differences. For example, women's executive processes may benefit more from exercise than men[45], and females demonstrate a higher fatty acid utilization and lesser fatigue following endurance running exercise[46]. In this study, although most of the effects induced by early-life exercise exhibited similar trends in males and females, there were subtle differences in the extent and specific aspects of these improvements. Specifically, early-life exercise increased BMD in females but not males in aged mice. We also notice that female mice subjected to early-life exercise gained weight during adulthood and aging. These female mice showed higher lean mass and healthier outcome. This phenomenon may be attributed to the metabolic patterns established by early-life exercise. A young Finns study revealed that youth physical activity might reduce body weight in youth but was not directly associated with adult abdominal obesity in either men or women[47]. Another finding demonstrated that juvenile 5-week climbing exercise established a muscle memory boosting the effects of adult exercise and led to leaner animals with lower body weight[48]. However, due to the complexity of the situation in humans and the inherent limitations of animal studies, more longitudinal studies involving human populations are needed to demonstrate the effects of early-life exercise on body weight in adulthood.

In conclusion, our study demonstrates that early-life exercise extends healthspan, but not overall lifespan, in both male and female mice. The improvements in cardiovascular function and muscle strength, as well as reductions in inflammation and frailty, underscore the importance of implementing early-life interventions to optimize long-term health outcomes. The identification of enhanced fatty acid metabolism as a potential underlying mechanism provides valuable insights into how exercise during critical developmental periods can shape lifelong health trajectories. Future studies are warranted to explore the mechanisms underlying the enduring long-term health effects of early-life exercise and to translate these findings to human populations.

Methods

Animal handling, welfare, and monitoring

All procedures involving animals were approved by Laboratory Animal Welfare and Ethics Committee of Fourth Military Medical University (Approval No. 20180303), in compliance with the Guide for the Care and Use of Laboratory Animals published by the US National Institutes of Health. Male and female C57BL/6J mice (4-week-old) were obtained from the Experimental Animal Center of Fourth Military Medical University and housed in a SPF room with controlled temperature (22–24 °C) and humidity (40–60%). All mice were housed in a room with a 12 h light-dark cycle, free access to food and water and fed ad-libitum with regular rodent chow (#DOSSYJY-001, DOSSY). Sterilized cages and bedding were changed weekly. Regular monitoring for infectious agents was performed, and all tests were negative throughout the study. The mice were randomly divided into 2 groups: those with early-life exercise (EXE), and those without early-life exercise (SED). Mice involved in lifespan analysis were kept in the same room housing 5 males or 5 females per cage in the same room but without mating throughout their entire life.

Animals were checked daily during experiments and were monitored for agility, basic awareness and general well-being. Body weight and food intake were regularly examined throughout their lifespan. We adhered to 3 R principles of animal welfare. All animals involved in our studies were well cared for and free from unnecessary pain or stress.

Exercise model

C57BL/6J mice (4-week-old) swam 90 min once daily for 5 days a week for 3 months. Mice were adapted to swimming training with a 30 min session on the first day. Sessions were then progressively increased to 90 min/day over a 1-week period. All exercise sessions took place during 19:00 p.m.–20:30 p.m. and the temperature of water was kept between 33–35 °C. The above training protocol was modified from a published article[49]. Tanks used for swimming were about 80 cm for length, 50 cm for width and 40 cm for height. Each tank contained 15–20 mice with same gender during swimming. The depth of water was 13–15 cm. Sedentary mice were age-matched and were kept in the same condition with 1–3 cm depth of water. Following 3 months of exercise training, mice were routinely housed without further training until death.

Survival

The principal endpoint of lifespan study was natural death. All mice were examined at least once daily. We recorded the age at which mice were found dead or selected for euthanasia. Euthanasia was performed on mice deemed unlikely to survive for the next 48 h and experiencing enormous discomfort. The criteria for euthanasia was based on an independent assessment by a veterinarian, which include severe lethargy, rapid weight loss (over two weeks >20%), severe distended abdomen and body condition score with signs of pain (grimace), inability to move despite the stimuli, severe ulcer or bleeding tumor, severe temperature loss with abnormal breathing rate. Mice were euthanized by intraperitoneal injection of not less than 150 mg/kg of sodium pentobarbital (Merck). A complete necropsy was performed on all mice and discernable tumors were recorded by a veterinarian and a clinician who were blinded to experimental conditions. The sample size was determined based on the ability to detect a 10% increase in lifespan with 80% power, using mean and standard deviations from published data[50].

Body composition

Measurements of lean and fat mass in live mice were acquired by NMR using the Minispec LF90 (Bruker Optics, Billerica, MA) based on Time-Domain NMR.

Multi-parameter metabolic assessment

Mouse metabolic rate was assessed by CLAMS lab animal monitoring system (Oxymax-CLAMS, Columbus Instruments, USA). Briefly, mice with free access to water were subjected to a standard 12 h light/12 h dark cycle, which consisted of a 24 h acclimation period followed by 48 h of sampling. Sampling time included a 24 h free access of food and 24 h fasting time followed. Sample air was passed through an O_2 sensor for determination of O_2 content. O_2 consumption was determined by measuring oxygen concentration in air entering the chamber compared with air leaving the chamber. All the sensor was calibrated before test. The concentrations of O_2 and CO_2 were monitored at the inlet and outlet of the sealed chambers to calculate oxygen consumption. Each chamber was measured for 30 s at 30-min intervals. Effective body mass was calculated by ANCOVA analysis. Respiratory quotient (RQ) was calculated as the ratio of VCO_2/VO_2, and total energy expenditure was calculated as $VO_2 \times (3.815 + 1.232 \times RQ)$, normalized to effective body mass, and expressed as kcal/h/kg $^{Eff.Mass}$. FO and CHO were calculated as $FO = 1.69\ VO_2 - 1.69 \times VCO_2$ and $CHO = 4.57 \times VCO_2 - 3.23 \times VO_2$ and expressed as g/d/kg$^{Eff.Mass}$ [51].

Frailty index assessment

The frailty index originally established by Whitehead et al.[52] are widely recognized as an effective index for mice frailty assessment. Deficits in body weight (g) and body surface temperature (°C) were scored based on deviation from reference values in young adult animals. The body surface temperature was assessed using an infrared thermometer (DELIXI Electric, China). Twenty-nine other items across the integument, physical/musculoskeletal, oscular/nasal, digestive/urogenital, and respiratory systems were scored on a scale of 0, 0.5, and 1 depending on the severity of the deficit in a blinded manner. Total score across the items was divided by the number of items measured to give a frailty index score between 0 and 1. It should be pointed out that for kyphosis frailty score from physical/musculoskeletal, inspection was needed for the mouse for its curvature of the spine or hunched posture. Then 0, 0.5, and 1 were used to score the kyphosis degree of mice: 0 means absent curvature, 0.5 means mild curvature and 1 means clearly hunched posture. The lower kyphosis frailty score means the less curvature of spine.

Micro-CT

The whole body of the mice was scanned using Quantum GX2 microCT Imaging System (PerkinElmer, USA). Scan parameters were set as follows: 90 kV, 80 μA and pixel size 288 μm. Based on the results of micro-CT scanning and reconstruction, the BMD was analyzed. Kyphosis index was calculated as the distance between the caudal margin of the last cervical vertebra to the caudal margin of the sixth lumbar vertebra (usually corresponding to the cranial border of the wing of the ilium) divided by a line perpendicular to this from the dorsal edge of the vertebra at the point of greatest curvature. The higher kyphosis index means less curvature of spine. Care was taken to avoid overextension or flexion of limbs.

Voluntary wheel running test

C57BL/6 mouse was randomly assigned to a running wheel-equipped cage (Vertical Wireless Running Wheel, Med Associates, USA). Free access to the wheel was allowed for every mouse in its cage. Running activity was monitored through a counter provided with each cage which counts whole counts of the activity wheel. For adaptation, all mice had access to wheels for 4 days before recording, and an average of running activity of the other 4 days were calculated as voluntary physical activity per day.

Glucose and insulin tolerance tests

Glucose tolerance test was performed by fasting the mice for 14 h overnight, followed by an intraperitoneal injection of glucose (1 g/kg). Insulin tolerance test (ITT) was performed by fasting mice for 4–6 h starting at lights on, and then injecting insulin (0.75 U/kg)

intraperitoneally[53]. Blood glucose levels were measured using a blood glucose meter and test strips (ACCU-CHEK, Roche, Swiss).

Ultrasonic imaging

Echocardiography was performed using a Vevo 2100 high-resolution in vivo imaging system (VisualSonics Inc., Toronto, Canada) to assess the cardiac function. Mice were anesthetized by 1% isoflurane to maintain stable heart rate and body temperature. M-mode and two-dimensional measurements were acquired to assess cardiac function. Systolic function was evaluated using the parasternal short-axis view. Diastolic function was assessed from the apical 4-chamber view by measuring E/A and E/E′ ratios. E wave (early filling) and A wave (atrial filling) were measured using pulse-wave Doppler mode between the tips of the mitral valve. The above training protocol was modified from a published article[54]. hcPWV was measured by capturing flow pressure waveforms generated by cardiac activity and arterial pulses and calculated by dividing the distance length by the transit time. CCA diameter was measured under pulse-wave Doppler mode.

Measurement of vascular function

Mice were euthanized and the descending aorta was carefully excised and placed in ice-cold physiological saline solution. The contractile force was recorded using a Powerlab Chart v 7.2.1 program (model 610 M, Danish Myo Technology, Denmark). Aortic rings were pre-contracted with phenylephrine (PE, 10^{-3} M, Sigma, USA). Endothelium-dependent vasorelaxation was evoked by acetylcholine (ACh, 10^{-9} to 10^{-3} M, Sigma, USA), while endothelium-independent vasorelaxation was evoked by cumulative sodium nitroprusside (SNP, 10^{-9} to 10^{-3} M, Sigma, USA). The above training protocol was modified from a published article[55].

Muscle performance tests

The forelimb grip strength of mice was measured using a grip-strength meter (BIO-GS3; Bioseb, Pinellas Park, FL, USA) with 5 measurements each mouse, and the average value was calculated. Prior to the test, the mice were acclimated to the rotarod with 3 trials every day for 3 days. The rotarod system (JLBehv-RRTG; Shanghai Jiliang Software Technology, Shanghai, China) accelerated from 4 rpm to 40 rpm over 5 min and maintained the maximum speed until the mice fell off. For the treadmill running capacity test, the mice were acclimated to the treadmill system (ZH-PT/5S, ZH, China) with 3 trials every day for 3 days. The treadmill was set at a 0° incline and initial speed of 5 m per minute. The speed was increased by 1 m per minute until exhaustion. Mice were motivated to run by a shock grid at the rear of the belt, and exhaustion time was recorded when the mice remained on the shock grid for more than 10 consecutive seconds. The above training protocol was modified from a published article[56].

Muscle force tests

Mice were anesthetized by 1.5% isoflurane before detaching the muscle, and maintenance of isoflurane was supplied during whole procedure. Then the TA muscle was gently detached and attached to the apparatus (Aurora Scientific, Aurora, ON, Canada). Optimal resting length (L_O) was determined through a series of twitches with each twitch separated by 30 s. L_O was the initial resting length where the muscle returned to after several pulses were administered. Force-frequency tests were assessed through electrical stimulations (10 V) at increasing frequency. Pause 5 min between stimulation bouts. Record force (in N) for each isometric contraction (P_O). After testing, specific force (N/cm^2) was determined for the TA by normalizing absolute force to physiological cross-sectional area, which was calculated as (P_ON)/[(muscle mass mg/1.06 mg/mm^3)/L_f mm]. 1.06 mg/mm^3 is the mammalian muscle density. $L_f = L_O \times 0.6$, where 0.6 is the muscle to fiber length ratio in TA muscle[57,58].

Respirometry of muscle fiber

Dissected gastrocnemius muscle strips were first immersed in ice-cold isolation solution (10 mM Ca-EGTA buffer, 0.1 µM free calcium, 20 mM imidazole, 20 mM taurine, 49 mM K-MES, 3 mM K_2HPO_4, 9.5 mM $MgCl_2$, 5.7 mM ATP, 15 mM phosphocreatine, 1 µM leupeptin, pH 7.1). Individual fiber bundles were then separated with two pairs of sharp forceps and then the fiber bundles were permeabilized for 30 min in 3 ml of ice-cold isolation solution with saponin (50 µg/ml). After chemical permeabilization, the tissue was rinsed twice for 10 minutes in chilled mitochondrial respiration medium MiR05 (0.5 mM EGTA, 3 Mm $MgCl_2.6H_2O$, 60 mM potassium-lactobionate, 20 mM taurine, 10 mM KH_2PO_4, 20 mM HEPES, 110 mM mannitol, 0.3 mM dithiothreitol, 1 g/l BSA, at pH 7.1). The fiber bundles were then transferred immediately into the respirometer (Oxygraph-2k; Oroboros Instruments, Innsbruck, Austria). Fiber samples were run in duplicate in the two-chamber system after calibration. All experiments were performed at 37 °C. Resting respiration was assessed by addition of octanoylcarnitine (1 mM) and malate (2 mM) in the absence of adenylates. OXPHOS capacity of fatty acid oxidation with octanoylcarnitine was achieved by addition of ADP (5 mM). OXPHOS capacity with convergence of physiological electron supply to the Q-junction through Complexes I and II was stimulated by addition of succinate (10 mM). OXPHOS capacity of CHO was assessed by addition of 5 mM pyruvate, ADP and succinate step by step[59]. All measurements were conducted blinded to treatment groups.

Complete blood counts

For complete blood counts, blood samples were obtained from the tail vein. The blood was collected into EDTA-coated collection tubes and analyzed using a Mindray BC-30 Vet hematology analyzer (Mindray, China).

ELISA

The following commercially available ELISA kits were used to measure protein levels in plasma: mouse Insulin Elisa kit (Cusabio, Wuhan, China) and mouse CRP Elisa kit (Cusabio, Wuhan, China). Relative levels of cytokines and chemokines in plasma were determined by using the Mouse cytokine array panel A array kit (ARY006, R&D Systems, Minneapolis, USA). The manufacturer's instructions were followed.

Histology and immunofluorescence

Tissues were collected after mice were anesthetized with 2% isoflurane. Fresh tissue was immediately fixed with 4% paraformaldehyde for 24 h. The tissue was then trimmed and dehydrated. Following OCT embedding, the tissue was sliced at a thickness of 10 µm. For gastrocnemius muscle, the region with the maximum cross-sectional area was sliced. H&E and Masson trichrome were used to evaluate tissue morphology and fibrosis, respectively. During the dewaxing process, environmentally friendly dewaxing transparent liquid (G1128, Servicebio) was used. The collagen volume fraction (%) was calculated as the ratio of collagen volume to fiber volume. For SA-β-Gal staining, sections were incubated with SA-β-Gal staining solution (9860, Cell Signaling Technology) overnight at 37 °C. After staining, slides were examined under a bright-field microscope (Zeiss).

For immunofluorescence, the sections were immersed in a 1X antigen retrieval solution (P0081, Beyotime) and then incubated at 95 °C for 10 min for antigen retrieval. Tissue sections were permeabilized by 0.2% Triton X (T8787, Sigma) for 10 min, and blocked in 1% bovine serum albumin for 20 min. The sections were incubated with primary antibodies overnight at 4 °C, including CD31 (ab9498, Abcam), CD11b (12-0112-82, Invitrogen) and laminin (ab11575, Abcam). Then slides were incubated with secondary antibodies conjugated with Alexa Fluor 488 (4408, Cell Signaling Technology) or Alexa Fluor 555

dyes (4413, Cell Signaling Technology) for 1 hour at room temperature. Nuclei were counterstained with DAPI (Invitrogen).

Imaging and quantification

The fluorescence was imaged using an inverted confocal microscope (Zeiss) or a slide scanner (OLYMPUS VS200). Endothelial integrity was quantified by calculating the ratio of CD31-positive aorta endothelial length to the entire aorta length. For quantification of the capillaries, all fibers in the slide were quantified by a blind observer. Capillaries were expressed as numbers per fiber. Automated quantitative analyses of capillary density were done by ImageJ software (v1.53). The images were converted into 8-bit grayscale images. For CD31 signal, the "Subtract Background" function (radius = 50 pixels) is applied to remove background noise, and then "Auto Threshold" (Otsu algorithm) is used to perform binary segmentation. The "Analyze Particles" module (particle size range: 5–100 μm^2, roundness 0.1–1.0) is used to identify capillary cross sections and exclude non-specific signals. The number of muscle fibers was then counted, and the capillary density was calculated. One tenth samples were randomly selected for manual review (ImageJ manual counting tool), and the results showed that the correlation coefficient between automatic and manual counting was $R^2 > 0.92$ (Pearson test). For confocal imaged results, an average value of each slide was calculated from five random microscopic fields by a blind observer.

Western blot

Proteins from tissues were quantified using a bicinchoninic acid protein assay kit (23225, Thermo Fisher). Western blot analysis was performed using standard procedures, which was detected using an enhanced chemiluminescence western blotting detection kit (32106, Thermo Fisher), and was quantified by scanning densitometry according to the manufacturer's protocols. Proteins were separated through electrophoresis and transferred to PVDF membranes. The membranes were incubated overnight at 4 °C with appropriate primary antibodies followed by incubation with the corresponding secondary antibodies at room temperature for 2 h. The primary antibodies were as follows: FASN (FASN, 3180S, Cell Signaling Technology), PPARγ coactivator-1α (PGC-1α, 2178S, Cell Signaling Technology), Atrogin 1 (67172-1-Ig, Proteintech), complex I (Invitrogen, 438800), complex II (Invitrogen, 459200), complex III (Invitrogen, 457125), complex V (Invitrogen, 459240), CD36 (18836-1-AP, Proteintech), carnitine palmitoyltransferase 1B (CPT1B, 22170-1-AP, Proteintech), carnitine palmitoyltransferase 1 A (CPT1A, 15184-1-AP, Proteintech), acyl-Coenzyme A dehydrogenase, long chain (ACADL, 17526-1-AP, Proteintech), p53 (10442-1-AP, Proteintech), p21 (28248-1-AP, Proteintech), p16 (554079, BD Pharmingen), phospho-p70S6K (Thr389) (9234, Cell Signaling Technology), total p70S6K (2708, Cell Signaling Technology), phospho-Akt (Ser473) (4060, Cell Signaling Technology), Akt (9272, Cell Signaling Technology), GAPDH (2118, Cell Signaling Technology) and α-tubulin (2125S, Cell Signaling Technology). α-Tubulin was used as a loading control. The original Western blots were provided in Source Data file.

Transcriptional profiling and analysis

Male mice used for transcriptional profiling were euthanized following an overnight fast. RNA was extracted from the heart, liver, gastrocnemius, and eWAT from male mice at different ages. Total RNA was extracted using Trizol reagent kit (Invitrogen, Carlsbad, CA, USA) according to the manufacturer's protocol. RNA quality was assessed on an Agilent 2100 Bioanalyzer (Agilent Technologies, Palo Alto, CA, USA) and checked using RNase free agarose gel electrophoresis. The cDNA/DNA/Small RNA libraries were sequenced on the Illumina sequencing platform by Genedenovo Biotechnology Co., Ltd (Guangzhou, China).

RNAs differential expression analysis was performed by DESeq2 software between two different groups. The genes with the parameter of p value below 0.05 were considered differentially expressed genes (DEGs). DEGs between young SED and old SED group were recognized as Aging DEGs, for these genes change due to aging. Exercise DEGs were identified by comparing between old SED and old EXE group. DEGs that increased with aging but decreased with exercise were categorized as "Rev-aging DEGs", while those changing in the same direction were categorized as "Pro-aging DEGs." DEGs classification was based on the established protocols outlined in a recent study[60].

PCA, GO, KEGG pathway, and SEA analyses were performed using the OmicShare tools, a free online platform for data analysis (http://www.omicshare.com/tools).

Statistical analysis

All values are presented as mean ± SEM. Repeats (n) mean experiments performed using distinct samples. Survival analyses were compared using Log-rank, Breslow, and Tarone-Ware test. The maximal lifespan was defined as the lifespan of the longest lived 5% of individuals. Daily Chi-square tests were used to assess differences between pairwise groups on each day of the lifespan[61]. Kolmogorov–Smirnov normality test was used to analyze the normal distribution of the data. Categorical data were compared by Chi-square test, and intergroup comparisons were conducted using two-sided t tests. For analyses involving multiple comparisons, one-way or two-way ANOVA was applied, as specified in the figure legends. Differences were considered significant when $P < 0.05$, with statistical results presented precisely in figures or as: * $p < 0.05$, and ** $p < 0.01$.

Reporting summary

Further information on research design is available in the Nature Portfolio Reporting Summary linked to this article.

Data availability

The accession number for the original mRNA sequencing data reported in this paper can be obtained from China National Center for Bioinformation with the accession code CRA025394. All other data are available within the Article and Supplementary Files. Source data are provided with this paper.

References

1. WHO. Global status report on physical activity 2022. (World Health Organization, 2022).
2. Kohl, H. W. et al. The pandemic of physical inactivity: global action for public health. *Lancet* **380**, 294–305 (2012).
3. Lee, I. M. et al. Effect of physical inactivity on major non-communicable diseases worldwide: an analysis of burden of disease and life expectancy. *Lancet* **380**, 219–229 (2012).
4. Chow, L. S. et al. Exerkines in health, resilience and disease. *Nat. Rev. Endocrinol.* **18**, 273–289 (2022).
5. Zhang, X. & Gao, F. Exercise improves vascular health: role of mitochondria. *Free Radic. Biol. Med* **177**, 347–359 (2021).
6. Guthold, R., Stevens, G. A., Riley, L. M. & Bull, F. C. Worldwide trends in insufficient physical activity from 2001 to 2016: a pooled analysis of 358 population-based surveys with 1.9 million participants. *Lancet Glob. Health* **6**, e1077–e1086 (2018).
7. Guthold, R., Stevens, G. A., Riley, L. M. & Bull, F. C. Global trends in insufficient physical activity among adolescents: a pooled analysis of 298 population-based surveys with 1.6 million participants. *Lancet Child Adolesc. Health* **4**, 23–35 (2020).
8. Zhang, J. et al. Burden of noncommunicable diseases among children and adolescents aged 10-24 years in China, 1990-2019: a population-based study. *Cell Rep. Med.* **4**, 101331 (2023).
9. Ren, J. et al. The aging biomarker consortium represents a new era for aging research in China. *Nat. Med.* **29**, 2162–2165 (2023).

10. Daines, C. L., Hansen, D., Novilla, M. L. B. & Crandall, A. Effects of positive and negative childhood experiences on adult family health. *BMC Public Health* **21**, 651 (2021).
11. Ford, C. A., Nonnemaker, J. M. & Wirth, K. E. The influence of adolescent body mass index, physical activity, and tobacco use on blood pressure and cholesterol in young adulthood. *J. Adolesc. Health* **43**, 576–583 (2008).
12. Yang, X., Telama, R., Viikari, J. & Raitakari, O. T. Risk of obesity in relation to physical activity tracking from youth to adulthood. *Med Sci. Sports Exerc.* **38**, 919–925 (2006).
13. da Silva, G. C. R. et al. Association of early sports practice with cardiovascular risk factors in community-dwelling adults: a retrospective epidemiological study. *Sports Med. Open* **9**, 15 (2023).
14. Zhang, N. et al. Early-life exercise induces immunometabolic epigenetic modification enhancing anti-inflammatory immunity in middle-aged male mice. *Nat. Commun.* **15**, 3103 (2024).
15. Telama, R. et al. Physical activity from childhood to adulthood: a 21-year tracking study. *Am. J. Prev. Med* **28**, 267–273 (2005).
16. Lopez-Otin, C., Galluzzi, L., Freije, J. M. P., Madeo, F. & Kroemer, G. Metabolic control of longevity. *Cell* **166**, 802–821 (2016).
17. Aging et al. Biomarkers of aging. *Sci. China Life Sci.* **66**, 1–174 (2023).
18. Englund, D. A., Zhang, X., Aversa, Z. & LeBrasseur, N. K. Skeletal muscle aging, cellular senescence, and senotherapeutics: current knowledge and future directions. *Mech. Ageing Dev.* **200**, 111595 (2021).
19. Lopez-Otin, C., Blasco, M. A., Partridge, L., Serrano, M. & Kroemer, G. Hallmarks of aging: an expanding universe. *Cell* **186**, 243–278 (2023).
20. Lamming, D. W. Quantification of healthspan in aging mice: introducing FAMY and GRAIL. *bioRxiv* (2024).
21. Warburton, D. E., Nicol, C. W. & Bredin, S. S. Health benefits of physical activity: the evidence. *Cmaj* **174**, 801–809 (2006).
22. Samitz, G., Egger, M. & Zwahlen, M. Domains of physical activity and all-cause mortality: systematic review and dose-response meta-analysis of cohort studies. *Int J. Epidemiol.* **40**, 1382–1400 (2011).
23. Farahmand, B., Broman, G., de Faire, U., Vågerö, D. & Ahlbom, A. Golf: a game of life and death–reduced mortality in Swedish golf players. *Scand. J. Med. Sci. Sports* **19**, 419–424 (2009).
24. Reimers, C. D., Knapp, G. & Reimers, A. K. Does physical activity increase life expectancy? A review of the literature. *J. Aging Res.* **2012**, 243958 (2012).
25. Garcia-Valles, R. et al. Life-long spontaneous exercise does not prolong lifespan but improves health span in mice. *Longev. Healthspan* **2**, 14 (2013).
26. Ji, N. et al. Aerobic exercise promotes the expression of ERCC1 to prolong lifespan: a new possible mechanism. *Med Hypotheses* **122**, 22–25 (2019).
27. Wu, G., Zhang, X. & Gao, F. The epigenetic landscape of exercise in cardiac health and disease. *J. Sport Health Sci.* **10**, 648–659 (2021).
28. Ashcroft, S. P., Stocks, B., Egan, B. & Zierath, J. R. Exercise induces tissue-specific adaptations to enhance cardiometabolic health. *Cell Metab.* **36**, 278–300 (2023).
29. Stanford, K. I. et al. Exercise before and during pregnancy prevents the deleterious effects of maternal high-fat feeding on metabolic health of male offspring. *Diabetes* **64**, 427–433 (2015).
30. Hernandez-Saavedra, D. et al. Maternal exercise and paternal exercise induce distinct metabolite signatures in offspring tissues. *Diabetes* **71**, 2094–2105 (2022).
31. Wang, K. et al. Epigenetic regulation of aging: implications for interventions of aging and diseases. *Signal Transduct. Target Ther.* **7**, 374 (2022).
32. McGee, S. L. & Hargreaves, M. Exercise adaptations: molecular mechanisms and potential targets for therapeutic benefit. *Nat. Rev. Endocrinol.* **16**, 495–505 (2020).
33. Palmer, A. K. & Jensen, M. D. Metabolic changes in aging humans: current evidence and therapeutic strategies. *J. Clin. Invest* **132**, e158451 (2022).
34. Zhou, Q., Yu, L., Cook, J. R., Qiang, L. & Sun, L. Deciphering the decline of metabolic elasticity in aging and obesity. *Cell Metab.* **35**, 1661–1671.e1666 (2023).
35. Yeo, D., Kang, C. & Ji, L. L. Aging alters acetylation status in skeletal and cardiac muscles. *Geroscience* **42**, 963–976 (2020).
36. Hornburg, D. et al. Dynamic lipidome alterations associated with human health, disease and ageing. *Nat. Metab.* **5**, 1578–1594 (2023).
37. Zeng, W. et al. Restoration of CPEB4 prevents muscle stem cell senescence during aging. *Dev. Cell* **58**, 1383–1398.e1386 (2023).
38. Murphy, A. J. & Febbraio, M. A. Immune-based therapies in cardiovascular and metabolic diseases: past, present and future. *Nat. Rev. Immunol.* **21**, 669–679 (2021).
39. Roh, K. et al. Lysosomal control of senescence and inflammation through cholesterol partitioning. *Nat. Metab.* **5**, 398–413 (2023).
40. Mutlu, A. S., Duffy, J. & Wang, M. C. Lipid metabolism and lipid signals in aging and longevity. *Dev. Cell* **56**, 1394–1407 (2021).
41. Papsdorf, K. & Brunet, A. Linking lipid metabolism to chromatin regulation in aging. *Trends Cell Biol.* **29**, 97–116 (2019).
42. Austad, S. N. & Fischer, K. E. Sex differences in lifespan. *Cell Metab.* **23**, 1022–1033 (2016).
43. Runolfsdottir, H. L., Sigurdsson, G., Franzson, L. & Indridason, O. S. Gender comparison of factors associated with age-related differences in bone mineral density. *Arch. Osteoporos.* **10**, 214 (2015).
44. Ji, H. et al. Sex differences in myocardial and vascular aging. *Circ. Res* **130**, 566–577 (2022).
45. Barha, C. K., Davis, J. C., Falck, R. S., Nagamatsu, L. S. & Liu-Ambrose, T. Sex differences in exercise efficacy to improve cognition: a systematic review and meta-analysis of randomized controlled trials in older humans. *Front. Neuroendocrinol.* **46**, 71–85 (2017).
46. Besson, T. et al. Sex differences in endurance running. *Sports Med.* **52**, 1235–1257 (2022).
47. Yang, X. et al. Testing a model of physical activity and obesity tracking from youth to adulthood: the cardiovascular risk in young Finns study. *Int J. Obes.* **31**, 521–527 (2007).
48. Eftestøl, E., Ochi, E., Juvkam, I. S., Hansson, K. A. & Gundersen, K. A juvenile climbing exercise establishes a muscle memory boosting the effects of exercise in adult rats. *Acta Physiol.* **236**, e13879 (2022).
49. Hou, Z. et al. Longterm exercise-derived exosomal miR-342-5p: a novel exerkine for cardioprotection. *Circ. Res* **124**, 1386–1400 (2019).
50. Mitchell, S. J. et al. Effects of sex, strain, and energy intake on hallmarks of aging in mice. *Cell Metab.* **23**, 1093–1112 (2016).
51. Grunewald, M. et al. Counteracting age-related VEGF signaling insufficiency promotes healthy aging and extends life span. *Science* **373**, eabc8479 (2021).
52. Whitehead, J. C. et al. A clinical frailty index in aging mice: comparisons with frailty index data in humans. *J. Gerontol. A Biol. Sci. Med Sci.* **69**, 621–632 (2014).
53. Bellantuono, I. et al. A toolbox for the longitudinal assessment of healthspan in aging mice. *Nat. Protoc.* **15**, 540–574 (2020).
54. Tan, Y. et al. Short-term but not long-term high fat diet feeding protects against pressure overload-induced heart failure through activation of mitophagy. *Life Sci.* **272**, 119242 (2021).
55. Yang, L. et al. SIRT3 deficiency induces endothelial insulin resistance and blunts endothelial-dependent vasorelaxation in mice and human with obesity. *Sci. Rep.* **6**, 23366 (2016).
56. Lou, J. et al. Exercise promotes angiogenesis by enhancing endothelial cell fatty acid utilization via liver-derived extracellular vesicle miR-122-5p. *J. Sport Health Sci.* **11**, 495–508 (2022).

57. Burkholder, T. J., Fingado, B., Baron, S. & Lieber, R. L. Relationship between muscle fiber types and sizes and muscle architectural properties in the mouse hindlimb. *J. Morphol.* **221**, 177–190 (1994).
58. Durumutla, H. B. et al. Comprehensive analyses of muscle function, lean and muscle mass, and myofiber typing in mice. *Bio Protoc.* **13**, e4617 (2023).
59. Kuznetsov, A. V. et al. Analysis of mitochondrial function in situ in permeabilized muscle fibers, tissues and cells. *Nat. Protoc.* **3**, 965–976 (2008).
60. Sun, S. et al. A single-cell transcriptomic atlas of exercise-induced anti-inflammatory and geroprotective effects across the body. *Innov.* **4**, 100380 (2023).
61. Newman, J. C. et al. Ketogenic diet reduces midlife mortality and improves memory in aging mice. *Cell Metab.* **26**, 547–557.e548 (2017).

Acknowledgements

We thank Prof. Rui Duan and Dr. Haiwang Shi from School of Physical Education and Sports Science, South China Normal University for the technical support. This work was supported by National Natural Science Foundation of China (31930055 to F.G.), National Key Research and Development Program of China (2023YFA1801200 to F.G.), and National Natural Science Foundation of China (32071169 to X.Z., 32371178 to X.Z., 32071108 to J.Li, and 32471184 to F.G.). Integrated Project of Major Research Plan of National Natural Science Foundation of China (92249303 to J.Liu) and National Natural Science Foundation of China (32171102 to J.Liu).

Author contributions

J.L., X.Z., and F.G. conceived and wrote the manuscript; M.F., M.L., J.Lou., G.W., N.Z., and Y.T. performed experiments; F.W., Y.Z., and C.S. were responsible for the mouse colony; M.F., M.L., J.L., X.Z., T.G., and L.Z. analyzed data; X.Z., J.Li., and F.G. secured funding. All authors have read and approved the final version of the manuscript and agree with the order of presentation of the authors.

Competing interests

The authors declare no competing interests.

Additional information

Supplementary information The online version contains supplementary material available at https://doi.org/10.1038/s41467-025-61443-4.

Correspondence and requests for materials should be addressed to Xing Zhang, Jiankang Liu or Feng Gao.

Peer review information *Nature Communications* thanks the anonymous, reviewers for their contribution to the peer review of this work. A peer review file is available.